Optimal design for survivable backbones with end-to-end and subpath wavebanding

Stefano Secci

Department of Network and Computer Science, ENST Paris, 37/39 rue Dareau, 75014 Paris, France
stefano.secci@enst.fr

Massimo Tornatore and Achille Pattavina

Department of Electronics and Information, Politecnico di Milano, Piazza Leonardo da Vinci, 32-20133 Milan, Italy
tornator@elet.polimi.it; pattavina@elet.polimi.it

Received May 17, 2006; revised September 28, 2006; accepted October 3, 2006; published December 11, 2006 (Doc. ID 70956)

We deal with the optimal design of a survivable optical mesh network supporting end-to-end and subpath waveband switching (WBS) in order to compare various WBS schemes according to a given cost function. An integer linear programming formulation is proposed to minimize the global network cost, which is expressed in terms of port cost, fiber cost, and propagation delay cost. We assume a single-layer multigranularity optical cross-connect (MG-OXC) node with a variable number of incoming fibers and a fixed number of wavelengths per waveband. The results show that on our case-study networks WBS with joint end-to-end and subpath wavebanding guarantees a gain of up to 22% and 85% in port number and global network costs, respectively.

OCIS codes: 000.1200, 060.0060.

1. Introduction

Because of continuous traffic growth, optical transport networks need to be upgraded, redesigned, and reconfigured to satisfy traffic increase and node addition. The lack of bandwidth on existing links pushes the operator to upgrade the existing installation or to ask for bandwidth from other operators in order to deploy new links or to modify the transmission rate on the existing ones, augmenting the number of wavelengths per fiber and the λ-channel rate.

Although switching nodes can be expanded with new shelves and cards, the number of required interconnections grows at a high pace, and new solutions are needed to make the optical circuit interconnects more scalable. As a matter of fact, a high number of wavelengths on network links raises the complexity of switching nodes: this complexity could be reduced if one could group more wavelengths channels into one single *waveband* to be switched as a unique channel. Thus only one entry and one exit port would be needed at the switching terminals, instead of installing as many ports as the number of wavelengths inside the waveband.

Waveband-switching (WBS) networks have been proposed as a possible solution to soothe the explosion of wavelength-driven channels, especially in geographical optical backbones. In this paper we face the problem of designing a minimal cost WBS backbone serving traffic volumes on the order of a terabit per second, where the objective is to dimension both the switching core nodes and the physical links. To comply with the strict availability requirements of most of today's applications, we allocate resources with a dedicated path protection strategy.

The design objective is the minimization of the network cost, composed of fiber costs, port costs, and light-path propagation delay costs. Usually in mesh backbone design this last factor is not considered, or at most the number of hops is minimized. This may result in an inaccurate choice, since a low hop number does not imply a short traveled distance; moreover, longer paths have higher signal attenuation, connection and splitting losses, and generally a worse optical signal-to-noise ratio value.

The paper is organized as follows: in Section 2 we review the most relevant papers on WBS network design; Section 3 describes synthetically the network model, while in Section 4 we depict an integer linear programming (ILP) approach to solving the dimensioning problem. Results and comments are reported in Section 5. Some conclusions are drawn in Section 6.

2. Literature Review

To the best of our knowledge, the dimensioning of a survivable WBS mesh architecture with a variable number of fibers per link has never been tackled in the literature. We will adopt the single-layer multigranularity optical cross-connect (MG-OXC) node described in Ref. [1]; as those authors point out, this node architecture guarantees a better signal quality and a smaller port number with respect to other node architectures. The authors delineate the WBS benefits and compare the architecture of multilayer and single-layer MG-OXC, showing the port allocation in the two cases. We will adopt the case with a variable number of wavebands per fiber and a fixed number of wavelengths per waveband, while in Ref. [1] the authors focus on the case with a fixed number of wavebands passing through a node.

In Ref. [2] the authors analyze how the traffic increase can be accommodated over an existing network having only OXC nodes, without considering fiber dimensioning and thus with a blocking switching node. Given the considered single-layer MG-OXC structure, the bandwidth unit to be switched can be only a wavelength, a waveband, or a fiber, and the existing wavelength cross-connect part cannot be overdimensioned. In Ref. [3] the authors assume a hierarchical optical node able to perform waveband and wavelength switching: only two kinds of port are taken into account, waveband switching and wavelength switching ports, and no fiber cross connection is considered. In Ref. [4] the authors propose an optimization method assuming a multilayer MG-OXC performing fiber, waveband, and wavelength conversion. Originally they considered wavebands that group λ channels with the same destination; this represents a strict constraint for wavebanding application.

It is worth noting that a single wavelength could be further partitioned (e.g., by means of time-division multiplexing), but *multigranular* optical switching would result in an extremely challenging network design problem. In Ref. [5] the authors propose an hybrid switching architecture employing both all-optical and electrical fabrics for performing, respectively, all-optical waveband switching and time-division multiplexing switching. That creates a very large design instance that they solved through mixed ILP only for small networks with a low number of wavelengths. In this paper we assume that traffic grooming of connections with below-wavelength granularity is performed only at the concentration level. We consider the routing of light paths, i.e., optical circuits that occupy an entire wavelength, and we deal with the problem of grouping these light paths into wavebands. Summarizing, the following grouping strategies can be employed in WBS networks [1]:

- *End-to-end grouping*: grouping of light paths with the same source–destination [5,3,2],
- *One-end grouping*: grouping of light paths with the same destination (or source) and different source (or destination) [4],
- *Subpath grouping*: grouping of light paths with a common subpath.

The application of subpath grouping would evidently be the best choice, even if the complexity for medium networks might be very high. On the other hand, end-to-end grouping and one-end grouping do not allow us to fully exploit the wavebanding capabilities. We will analyze, for the first time to our knowledge, the case of joint end-to-end grouping and subpath grouping.

3. Network Model

In this section we synthetically describe our network model: physical infrastructure, traffic nature, and node architecture.

3.A. Physical Architecture

The physical topology is characterized by a set of nodes identifying the sites where switching equipment is installed, and by a set of unidirectional interconnection arcs

between those nodes. The number of fibers per arc is not predefined and has to be dimensioned. We call a set of fibers in the same direction and on the same arc an optical link. The fibers are equipped with $W=16$ wavelengths, each with a channel capacity of $C_{ch}=10$ Gbits/s.

3.B. Traffic Nature

The traffic matrix consists of static connection requests (CRs) between two nodes whose bit rate represents an aggregated flow, coming, e.g., from synchronous digital hierarchy (SDH) rings at the concentration level. The CR traffic is determined through a gravitational model [6]: the traffic between two sites is directly proportional to the product of the population values of the metropolitan areas [7] and inversely proportional to the square of the distance between the sites; the resulting value is opportunely scaled to obtain a global requested traffic volume on the order of terabits per second as described in Section 5. Thus the traffic matrix is symmetric, and the virtual topology is fully meshed.

We assume three main bit-rate classes for light paths; a CR is mapped over one or more light paths of different bit-rate classes to obtain the best rounding-up value. So the gap between the required transport capacity and the allocated capacity will be as small as possible. Let us indicate by Z_h the bit rate of a light path of class h, $h \in H = \{1,2,3\}$; the number of light paths of class h (LP-h) per CR is the minimum possible to accommodate the CR traffic. We assume $Z_1=C_{ch}=10$ Gbits/s for LP-1, which has the transport capacity of a wavelength, $Z_2=4Z_1=40$ Gbits/s for LP-2, which has the transport capacity of a waveband grouping $R=4$ wavelengths, and $Z_3=WC_{ch}=160$ Gbits/s for LP-3, which has the transport capacity of a fiber (also called *multiwaveband* from now on). The three main classes thus use as the transport unit, respectively, the wavelength, the waveband, and the fiber. For example, considering $CR_1=195$ Gbit/s and $CR_2=30$ Gbit/s, then CR_1 would be mapped onto 1 LP-3 and 1 LP-2 (instead of 1 LP-3 and 4 LP-1), and CR_2 onto 3 LP-1 (instead than 1 LP-2). The mapping of the traffic matrix over the bit-rate classes creates the set of LPs to be routed.

Using the previous bit-rate classes, we obtain a correspondence with the bit-rates of SDH and optical transport network (OTN) interfaces [8] as shown in Table 1. For example, a backbone may receive traffic from a concentration level based mainly on SDH rings; an LP-1 may serve the traffic from and to an add–drop multiplexer (ADM) of a STM-64 ring, or the aggregated traffic from and to ADMs of four STM-16 rings; similarly, LP-2 and LP-3 may accommodate higher bit-rates or may be rented to other operators.

3.C. Node Architecture

We adopt the single-layer MG-OXC described in Ref. [1] and illustrated in Fig. 1; it has one common optical switching fabric, which includes three logical parts: the fiber cross connector (FXC), the waveband cross connector (BXC), and the wavelength cross connector (WXC); we will suppose full cross-connection features and thus no continuity constraint. At the input interface demultiplexing operations are performed and local fibers, wavebands, or wavelengths are added, while at the output interface multiplexing and dropping are performed.

The incoming fibers that bypass the local site can be directly switched through FXC, without any wavelength and waveband demultiplexing; each of these bypassed fibers requires two ports, one at the input and one at the output stage. Also, locally dropped fibers require two ports each, one port at the input stage and one drop port at the output stage. The remaining incoming fibers transport one or more wavelengths or wavebands to be either bypassed or dropped at local site. These fibers are firstly demultiplexed in their wavebands. Then the bypassed wavebands (those grouping wavelengths that are dropped at the local site) can be directly switched by BXC and

Table 1. Mapping of SDH and OTN Interfaces on LP Bit-Rate Classes

Light-Path Classes	Bit Rate	SDH Tributary	OTN Tributary
LP-1	$C_{ch}=10$ Gb/s	STM-64	OTU-1
LP-2	$4C_{ch}=40$ Gb/s	STM-256	OTU-2
LP-3	$WC_{ch}=160$ Gb/s	STM-1024	—

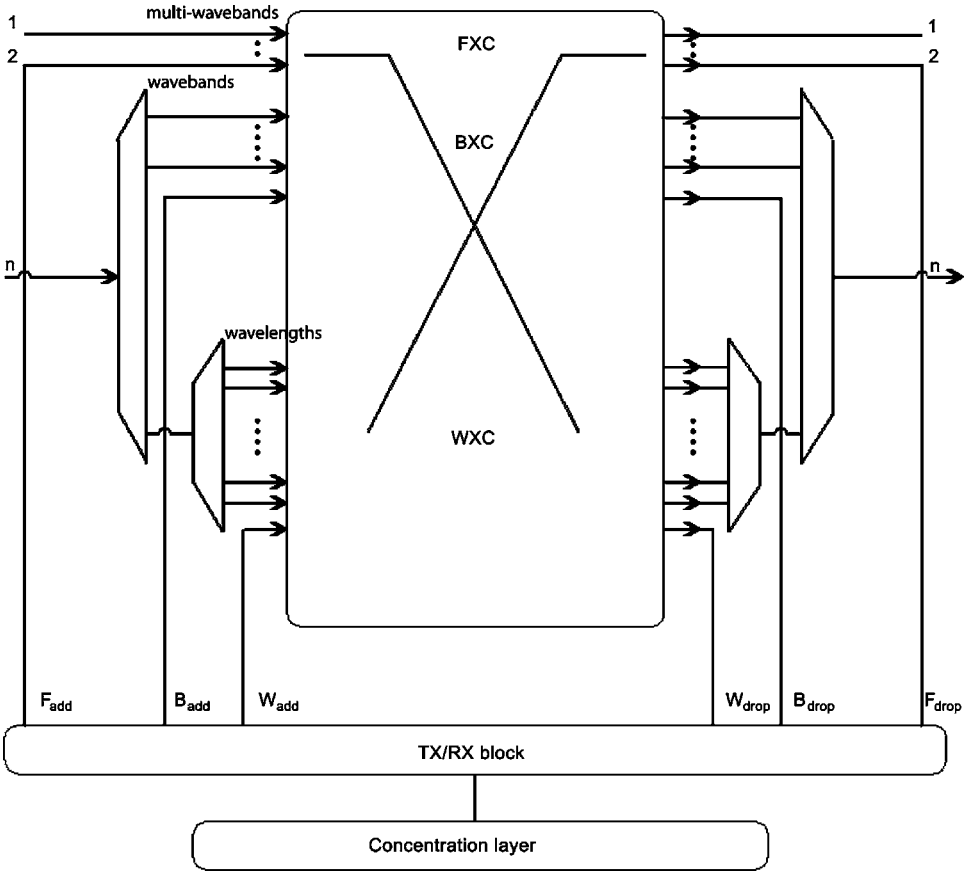

Fig. 1. Single-layer MG-OXC.

require two ports each. Also, locally dropped wavebands require two ports each, one at the input stage and one drop port at the output stage.

The remaining wavebands transport one or more wavelengths to be either bypassed or dropped at the local site. Again, both the wavelengths bypassed through the WXC and the wavelengths dropped at the WXC output require two ports each. The same mechanism applies for locally added fibers, wavebands, and wavelengths: one add port at input stage, and one port at output stage.

It is worth noting that the wavelength continuity constraint strongly limits the benefits of wavebanding: as a matter of fact, in most of the previous work on wavebanding this constraint has not been included in the model. Indeed, the wavelength continuity constraint would implicitly imply a waveband continuity constraint, decreasing the chance for efficient subpath wavebanding. The application of these constraints would produce an overdimensioned backbone with many unused wavelengths and wavebands, low network utilization, and a large amount of idle capacity. Moreover, the application of wavelength continuity constraint would produce more complex optimization problems as the authors of Ref. [9] pointed out. Further work is needed to develop heuristics to evaluate the effect of the wavelength continuity constraint on wavebanding effectiveness.

3.C.1. End-to-End Grouping Example

Let us consider a simple example to clarify the node architecture and to show how we can perform port allocation by end-to-end wavebanding. Consider the case that at a given site we have six fibers of 16 wavelengths entering the site, and six exiting it. If we use basic OXCs, every one of the input–output fibers would be demultiplexed–multiplexed in–from all its wavelengths. In this case, the OXC contains $6\times16\times2=192$ ports. Suppose now that the six entering fibers transport four LP-3, seven LP-2, and four LP-1, among which one LP-3, one LP-2, and one LP-1 must be dropped, and one LP-3, one LP-2 and one LP-1 must be added. Thus both the incoming and the outgoing fibers are fully used; the four LP-3 occupy one fiber each, and the seven LP-2 and the four LP-1 are transported through two fibers. The required number of input

ports for the FXC is thus 4+1=5. Two fibers are demultiplexed into wavebands; between the eight demultiplexed wavebands, seven (the LP-2) are switched through a BXC with 7+1 ports (one port for the locally added LP-2). The eighth waveband is demultiplexed into four wavelengths, which are switched through WXC with 4+1 ports (1 port for the locally added LP-1). At the output interface the number of ports is the same as at the input interface; we have thus 4+7+4=15 ports for bypass LPs and 1+1+1=3 ports for the dropped LPs. Globally, we need a total of 36 ports; that is exactly twice as many as the number of bypassed, dropped, or added LPs, while with an OXC we would need 192 ports.

3.C.2. Addition of Subpath Grouping

Let us now consider the case that the 6 fibers transport 1 LP-3, 19 LP-2, and 4 LP-1 (dropped LPs remain 1 LP-3, 1 LP-2, and 1 LP-1). With a MG-OXC we would need $2\times(1+19+4+1+1+1)=54$ ports instead of 36. Similarly, if we have 4 LP-3, 5 LP-2, and 12 LP-1, we need $2\times(4+5+12+1+1+1)=42$ ports instead of 36. A possible method to further reduce the number of ports is to switch, as a single entity, groups of LPs that bypass a switching node even if they do not belong to the same end-to-end path. The objective is to group, where possible, those LPs of type 1 and 2 that bypass a node into, respectively, wavebands and multiwavebands: e.g., four LP-1 can be grouped into one waveband, and, similarly, four LP-2 can be grouped into one multiwaveband. This new functionality makes it possible to apply the so-called subpath grouping; it requires identifying for every hop all the LPs that bypass it and could form the local wavebands and *local multiwavebands*. Moreover, consider the case in which at a given site there are two LP-2 that have not been grouped into a multiwaveband, since no associable LP-2 was available, and two wavebands creating grouping LP-1. These entities can further be grouped in what we call a *heterogeneous local multiwaveband*.

3.D. Switching Hierarchy

An agreed taxonomy is needed to unequivocally identify the MG entities that are switched in a MG-OXC. From now on we employ the following classifications, simplified in Fig. 2:

- *End-to-end wavelength*: a wavelength used by an end-to-end light path of the first bit-rate class (LP-1).
- *Waveband*: a set of (let us say R) wavelengths grouped as an
  - *End-to-end waveband*: an end-to-end light path of the second bit-rate class (LP-2) or a
  - *Local waveband*: a set of R end-to-end lightpaths (LP-1) that bypass a switching site.
- *Multiwaveband*: a set of R wavebands grouped as a
  - *End-to-end multiwaveband*: end-to-end lightpath of the third bit-rate class (LP-3), or a
  - *Local multiwaveband*: a group of R end-to-end wavebands bypassing a switching site, or a
  - *Heterogeneous local multiwaveband*: a group of end-to-end wavebands and local wavebands.

This corresponds to fiber switching.

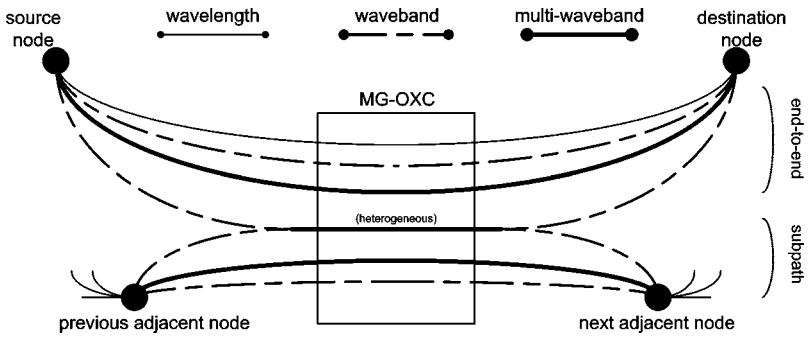

Fig. 2. MG channel entities.

In the following, we model and analyze the following four cases:
1. *OXC:* basic OXC without any wavebanding;
2. *MG-OXCs:* MG-OXC with end-to-end wavebanding and multiwavebanding;
3. *MG-OXCh:* local wavebanding and multiwavebanding added to MG-OXCs;
4. *MG-OXCc:* heterogeneous local multiwavebanding added to MG-OXCh.

4. Integer Linear Programming Optimization

The purpose of our ILP model is to opportunely allocate resources (fibers, ports) and assign them to light paths to guarantee fast communications (i.e., with low propagation delay); the outputs are the optimal light-paths routes and the wavebands and multiwavebands that have to be created locally and end-to-end.

In other work on WBS, the usual design objective contains only the global number of ports. We exploit a more refined cost function (originally proposed in Ref. [6] according to the suggestions of a network operator), which captures the global network cost as a combination of distinct cost contributes. The new model of network cost has been expressed as the sum of the cost of the fibers to be installed, and of the ports at switching nodes (real costs), and of the cost due to propagation delays (virtual cost). The switch fixed cost is not considered because it has been considered negligible with respect to port cost. The propagation delay unitary cost of a LP is directly proportional to its bit rate and to the traveled distance. Note that the propagation delay cost is a virtual cost, and it does not represent the real propagation delay; it is employed to allow the assignment of short routes to light paths, giving the priority to light paths with high bit rates: consider that a crucial issue to be solved for selling voice over IP and video services with a high quality of service is to guarantee the lower possible delay in the transmission systems; such services should require LPs of high classes in our model, and these must have priority in getting the bandwidth over shorter paths.

We adopt a dedicated path protection strategy; for every working light path (w-LP) we allocate a protection bandwidth for its protection light path (p-LP), which must be link disjoint [10]. To the best of our knowledge, this is the first time dedicated protection has been applied in a design problem with WBS. In particular, in the case of 1:1 dedicated path protection it makes sense to enable a shorter path for w-LPs and a longer path for p-LPs to be used in case of failure along the working path. For this reason the optimization problem should give priority to w-LPs in the contention for shortest paths.

In the following we discuss a set of ILP formulations to solve the design problem with wavebanding according to network model, constraints, and node architecture seen in Section 3. The input data are the set of LPs to be routed and the preassigned physical topology. The outcome of the optimization process is the number of fibers per link to install, the number of ports needed on each switching node, and the assignment for each LP to the unidirectional optical links to be traversed. We report the ILP formulations for all the four wavebanding schemes; the notation is reported in Table 2.

4.A. Integer Linear Programming Formulation

$$\min G(\bar{x}) = \sum_{(p,h,l)_w} \sum_{(i,j)} \beta Z_h d_{i,j} x_{i,j}^{p,h,l} + \sum_{(p,h,l)_p} \sum_{(i,j)} \sigma\beta Z_h d_{i,j} x_{i,j}^{p,h,l} + \sum_{(i,j)} WF d_{i,j} l_{i,j} + P(\bar{x}) \quad (1)$$

subject to

$$\sum_{j\in N} x_{i,j}^{p,h,l} - \sum_{j\in N} x_{j,i}^{p,h,l} = \begin{cases} 1 & \text{if } i = s(p) \\ -1 & \text{if } i = d(p) \\ 0 & \text{otherwise} \end{cases} \quad \forall\, i \in N, \quad \forall\, (p,h,l)_{wp}, \quad (2)$$

$$x_{i,j}^{p,h,l} + x_{i,j}^{p,h,l+L_h} \leq 1 \quad \forall\, (i,j), \quad \forall\, (p,h,l)_w, \quad (3)$$

$$\sum_{(p,h,l)_{wp}} Z_h x_{i,j}^{p,h,l} \leq WC_{\text{ch}} l_{i,j} \quad \forall\, (i,j), \quad (4)$$

Table 2. Notation

$G(N,\epsilon_P)$	Physical topology oriented graph; N is the set of nodes, ϵ_P the set of arcs
$(i,j)\in\epsilon_P$	Arc, or optical link, between the node i and the node j
d_{ij}	Distance (km) between node i and node j
C_{ch}	=10 Gbit/s, capacity of a wavelength-channel
W	=16, number of wavelengths per link
F	Reference fiber cost in unit of length (km) and of wavelength
P	Unitary port cost
β	Propagation delay cost in unit of traffic and of traveled distance
σ	Scaling factor for the propagation delay cost of the p-LPs, $0<\sigma<1$
T	$\subset N\times N$, set of pairs of different nodes; the entry $p\in T$ identifies a CR
$s(p)/d(p)$	Source–destination node of pair p
Z_h	Traffic bit rates (Gbit/s) for classes of traffic h, $h\in H=\{1,2,3\}$
R	Number of wavelengths/wavebands forming a waveband/multi-waveband. We set $W=R^2$ to have $Z_h=RZ_{h-1}, h<3$. We will use $R=4$.
(p,h,l)	Triple identifying the l^{th} LP of class h between the nodes of pair p
L_h	Maximum number of LP-h per connection request p
$(p,h,l+L_h)$	Triple identifying the p-LP of w-LP (p,h,l)
$(p,h,l)_w$	Set of all w-LPs, $p\in T$, $h\in H$ and $0<l\leqslant L_h$
$(p,h,l)_p$	Set of all p-LPs, $L_h<l\leqslant 2L_h$
$(p,h,l)_{wp}$	Set of all LPs, $0<l\leqslant 2L_h$
$x_{i,j}^{p,h,l}$	Indicates whether the LP (p,h,l) passes over the link (i,j)
$l_{i,j}$	Number of fibers to install on the link (i,j)

$$x_{i,j}^{p,h,l}\in\{0,1\},\quad l_{i,j}\in N. \tag{5}$$

Constraint (1) expresses the minimization of the total network cost due to propagation delays, fibers, and switching ports [$P(\bar{x})$ varies for the different cases]. The propagation delay cost associated with the p-LPs is scaled by σ to avoid competition for the best path between a w-LP and its p-LP.

Constraint (2) is the traffic conservation constraint, requiring that the flow leaving node i be balanced by the entering flow, except for the source (destination) node.

Constraint (3) imposes the protection constraint, which requires that a p-LP cannot be routed on the same link where the correspondent w-LP is routed.

Constraint (4) imposes the capacity constraint for every link of the network: the global bit rate of the LPs traversing a link (i,j) must be less than the capacity offered by the $l_{i,j}$ fibers to be allocated on that link.

Constraint (5) imposes the binary constraint for x and the integer constraint for l.

$P(x)$ changes according to the various schemes described in Section 3.D. In the following sections we describe how to evaluate this cost function. Note that in the case of locally added or dropped LPs an additional add–drop port is not needed, since it is replaced by an entrance–exit port.

4.B. OXC Case: No Wavebanding

If we assume a switching node composed of OXCs with no wavebanding functionalities, then every fiber has to be demultiplexed in all its tributary wavelength signals and thus requires $2W$ ports of unitary cost P to be installed; thus

$$P(\bar{x}) = P_1(\bar{x}) = \sum_{(i,j)} 2PWl_{i,j}. \tag{6}$$

4.C. MG-OXCs Case: End-to-End Wavebanding

If we include end-to-end waveband switching, the number of required ports at a switching node is equal to the double the number of LPs traversing it, which can be end-to-end wavelengths, wavebands, and multiwaveband channels; so

$$P(\bar{x}) = P_2(\bar{x}) = \sum_{(i,j)} \sum_{(p,h,l)_{wp}} 2Px_{i,j}^{p,h,l}. \tag{7}$$

4.D. MG-OXCh Case: End-to-End and Subpath Wavebanding

Considering local wavebands and multiwavebands in addition to end-to-end wavebands and multiwavebands, the number of ports per fibers is obtained from the number of ports needed in the MG-OXCs case minus the number of ports saved thanks to local wavebands and multiwavebands.

The global port cost is calculated with the following notation and constraints.

$(i,j,k) \in N \times N \times N$, $(i,j) \in \epsilon_P$, $(j,k) \in \epsilon_P$, $k \neq i$, is a one-hop arc.

$f_{i,j,k}^{p,h,l}$ is an integer variable set to 1 if the LP (p,h,l) passes over the one-hop arc (i,j,k), or to 0 otherwise.

$s_{i,j,k}^{h}$ is the number of one-hop wavebands ($h=1$) or multiwavebands ($h=2$) over the one-hop arc (i,j,k).

$$2f_{i,j,k}^{p,h,l} \leqslant x_{i,j}^{p,h,l} + x_{j,k}^{p,h,l} \quad \forall (i,j,k), \quad \forall (p,h,l)_{wp,h\in\{1,2\}}, \tag{8}$$

$$Rs_{i,j,k}^{h} \leqslant \sum_{(p,h,l)_{wp}} f_{i,j,k}^{p,h,l} \quad \forall (i,j,k), \quad \forall h \in \{1,2\} \subset H, \tag{9}$$

$$f_{i,j,k}^{p,h,l}, s_{i,j,k}^{h} \in N, \tag{10}$$

$$P(\bar{x}) = P_3(\bar{x}) = P_2(\bar{x}) - 2RP \sum_{(i,j,k)} \sum_{h\in\{1,2\}} s_{i,j,k}^{h}. \tag{11}$$

4.E. MG-OXCc Case: Addition of Heterogeneous Subpath Wavebanding

Now we introduce the heterogeneous local multiwaveband, which is able to group end-to-end wavebands (not already grouped in multiwavebands) with existing local wavebands.

The global port cost is calculated with the following notation and constraints.

$m_{i,j,k}$ is the number of heterogeneous local multiwavebands over the one-hop arc (i,j,k).

$g_{i,j,k}^{h}$ is the final number of local wavebands ($h=1$) and multiwavebands ($h=2$) over (i,j,k).

$$Rm_{i,j,k} \leqslant \sum_{(p,h,l)_{wp}}^{h=2} f_{i,j,k}^{p,h,l} - Rs_{i,j,k}^{2} + s_{i,j,k}^{1} \qquad \forall (i,j,k), \tag{12}$$

$$g_{i,j,k}^{1} = s_{i,j,k}^{1}, g_{i,j,k}^{2} = s_{i,j,k}^{2} + m_{i,j,k} \qquad \forall (i,j,k), \tag{13}$$

$$g_{i,j,k}^{h}, m_{i,j,k} \in N, \tag{14}$$

$$P(\bar{x}) = P_4(\bar{x}) = P_2(\bar{x}) - 2RP \sum_{(i,j,k)} \sum_{h\in\{1,2\}} g_{i,j,k}^{h}. \tag{15}$$

In the OXC and MG-OXC cases, the variable number is equal to $|N|^2(a|N|+1)$, and the constraint number is equal to $|N|^2(1+\frac{3}{2}a)$, where a is the average number of LPs per node and $|N|$ the number of nodes, assuming a full meshed physical topology (worst case). The introduction of the subpath grouping increases the complexity by a factor of N: in particular, the MG-OXCh case introduces $|N|^3(2+|N|a)$ additional constraints and variables, and MG-OXCc adds $3|N|^3$ constraints and variables.

5. Results

We consider the three case-study networks depicted in Fig. 3: the EON, the NSFNET, and a six-node backbone extracted from the EON core that we will call EONc. The NSFNET has 14 nodes and 44 unidirectional arcs. The EON is a more interconnected backbone with 19 nodes and 78 arcs, and the EONc has 6 nodes and 18 arcs. We analyze these three networks loaded by three different traffic volumes; the global traffic load is set equal to the global transport capacity of the considered backbones, if equipped with 1, 2, or 3 fibers per unidirectional arc. Then the total traffic is distributed among all the node couples in the network according the gravitational model introduced in Section 2.

Cost values are expressed in unit of fiber cost F [6]: $P/F=150$, $\beta/F=0.1$. We set $\sigma=0.9<1$. To solve the ILP problems we used the CPLEX software tool based on the branch-and-bound method and, as computational platform, a 2.4 GHz processor workstation equipped with 16 GBytes of available RAM memory. The optimization problem can be solved quickly for low traffic loads, especially in the cases without subpath grouping; however, solutions for MG-OXCh and MG-OXCc are more difficult to obtain. For example, the number of variables and constraints goes from 31,196 and 25,532 for the NSFNET-1–OXC case to 139,960 and 239,324 for the NSFNET-3–MG-OXCc case (NSFNET-x stands for x fibers per arc global traffic load).

We fixed a time limit of 36 h to achieve the solution: when the solver does not reach the optimal solution within this limit, then, if at least a feasible integer solution reasonably close to the optimal solution is available, we report it; otherwise we report that the solution is not available (NA). This happens to NSFNET and EON in the most complex subpath wavebanding cases. We have, however, enough results over the EONc network to estimate the effectiveness of WBS in all the WBS schemes.

Note that from the result of the optimization instance we can retrieve the lightpath routes, the wavebands, and multiwavebands to be formed locally and end to end, and thus the node structure according to the architecture shown in Section 3: every node will be characterized by a different configuration of the input and output interfaces in terms of enabled ports and switching interconnection scheme.

Tables 3 and 4 contain, respectively, the objective values of network cost and the number of ports for the three networks under different traffic loads. The first table is useful to observe how the total network cost is affected by the application of wavebanding; the second table is a better indicator of how the different waveband grouping methods determine the ports to enable in the network.

As expected, adding WBS capabilities to the switching nodes allows for an increasing reduction of the network cost as well as of the port number. In particular, the most significant gain is already achieved by means of end-to-end wavebanding (MG-OXCs case): in this case, grouping connections relative to the same source–destination couple results in a great advantage, especially for high network loads when, according to our traffic model, the LP-2 and LP-3 are dominant with respect to LP-1.

WBS performance can be further improved by also grouping connections that belong to different end-to-end connections: in Tables 3 and 4 we demonstrate that the effect of subpath grouping can be still significant, especially for lower traffic loads: results show that the MG-OXCh case induces a small decrease in network cost, yet a more significant gain in ports, especially for lower traffic traffic loads; as a matter of fact, the subpath grouping tends to perform better when the network has more residual capacity and when many connections with low granularity are available and can be grouped: these two situations are more likely to emerge for low traffic loads. Moreover, dense topologies may benefit more from subpath grouping: in full-meshed

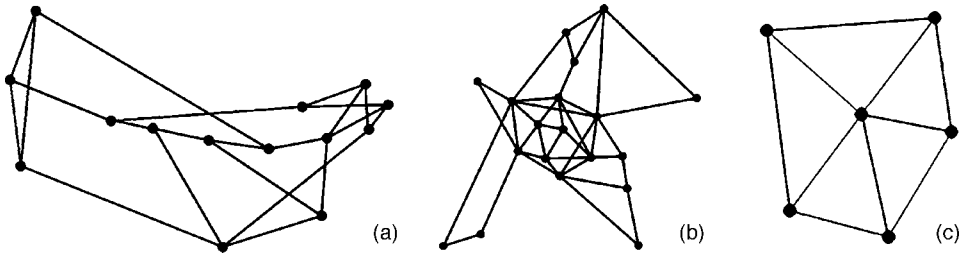

Fig. 3. Topology types: (a) NSFNET, (b) EON, (c) EONc.

Table 3. Objective Values (in thousands) under Different Traffic Volumes and Cases

	NSF			EON			EONc		
Load Case	1	2	3	1	2	3	1	2	3
OXC	10656	19257	28021	8945	14970	20970	1192	2282	3281
MG-OXCs	10039	17840	25741	8062	12985	17975	986	1782	2533
MG-OXCh	9781	17479	25350	NA	NA	NA	969	1772	2527
MG-OXCc	NA	NA	NA	NA	NA	NA	967	1767	2515

Table 4. Number of Allocated Ports under Different Traffic Volumes and Cases

	NSF			EON			EONc		
Load Case	1	2	3	1	2	3	1	2	3
OXC	7904	14240	20992	11456	20256	28896	1984	3968	5760
MG-OXCs	3806	4762	5416	5370	6902	8234	544	636	772
MG-OXCh	3197	2796	4454	NA	NA	NA	492	558	728
MG-OXCc	NA	NA	NA	NA	NA	NA	476	551	724

networks we believe that we can perform better subpath wavebanding than in ring topologies, for example. In Ref. [1] authors observed that the introduction of subpath grouping may induce longer light-path routes, because the joint enforcement of capacity constraints and minimization of WBS ports could lead to rerouting of connections over less effective paths. Let us point out that, in our work, this trade-off is solved according to the minimization of a different network cost.

Finally, in the MG-OXCs case we added the heterogeneous local multiwavebanding functionality, which grants a further, yet very small additional reduction in port number and network cost; remarkable savings by heterogeneous local grouping may be achieved only in networks with few LPs, mainly of lower bit-rate classes. In the MG-OXCs case, the design problem becomes very challenging, and we could solve it only for the EONc topology. Since network design and management becomes more difficult to tackle, the operator of each network should decide according to planning requirements whether heterogeneous wavebanding is a feasible choice to be implemented in the network.

Comparing the results on the three network topologies, we can observe that, in percentage, the global cost and port number reduction is smaller in NSFNET and EON than in EONc; this difference is related to the larger arcs length in NSFNET and EON: longer arcs imply larger fiber costs, while the port cost is not affected by the geographical dimension. As a consequence, wider networks tend to have higher fiber cost with respect to port cost in our model. The application of WBS reduces the cost amount due to ports, modifies the global propagation delay cost because light paths are deflected from the shortest path to increase WBS, while the fiber cost is not (at least directly) reduced by WBS.

In Fig. 4 we show the percentage savings of the various forms of WBS with respect to the OXC case for the different traffic loads in the EONc case. In Fig. 4(a) we report the global cost percentage decrease: from OXC to MG-OXCs, the objective reduces rapidly to 22% with the EONc topology. This reduction increases for higher values of traffic load: the LP-1 number is stable in the three traffic scenarios, and so is the number of formed wavebands; in contrast, the LP-2 number increases significantly with the number of formed multiwavebands. In Fig. 4(b) we report the percentage reduction of port numbers. Considering the case with lower traffic, MG-OXCs already reduces the port number already by more than 70%, and this reduction keeps increasing to greater than 75% for the MG-OXCh and MG-OXCc cases. For high traffic loads the saving is even more consistent, reaching 88%.

In Fig. 5 we illustrate how the global network cost is distributed among its components (fibers, ports, and propagation delays). Without WBS, the port cost represents about 26% of the global cost. The introduction of end-to-end wavebanding is able to reduce the port cost share to 4.57%: this share shows very small additional decreases with subpath wavebanding. Note that the share of cost due propagation delay increases when passing from MG-OXCs to MG-OXCh: this confirms that subpath grouping may imply longer paths for the grouped LPs.

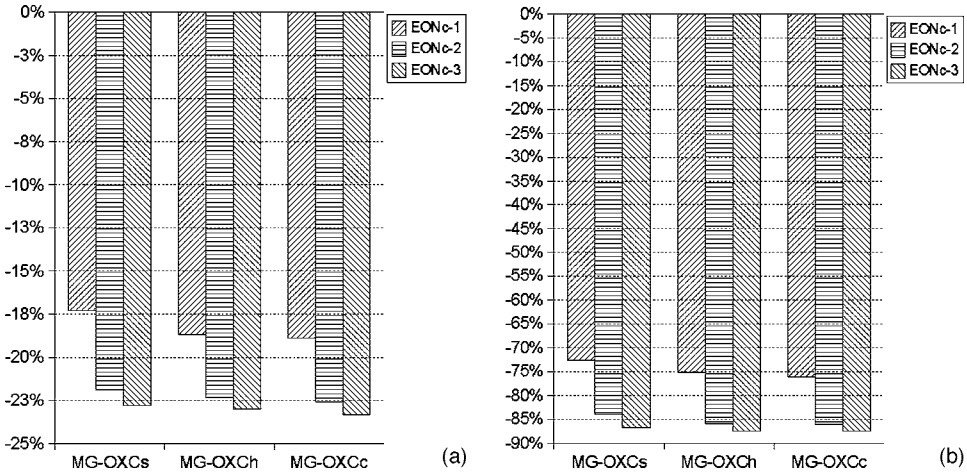

Fig. 4. (a) Objectives and (b) port percentage reduction for EONc topology.

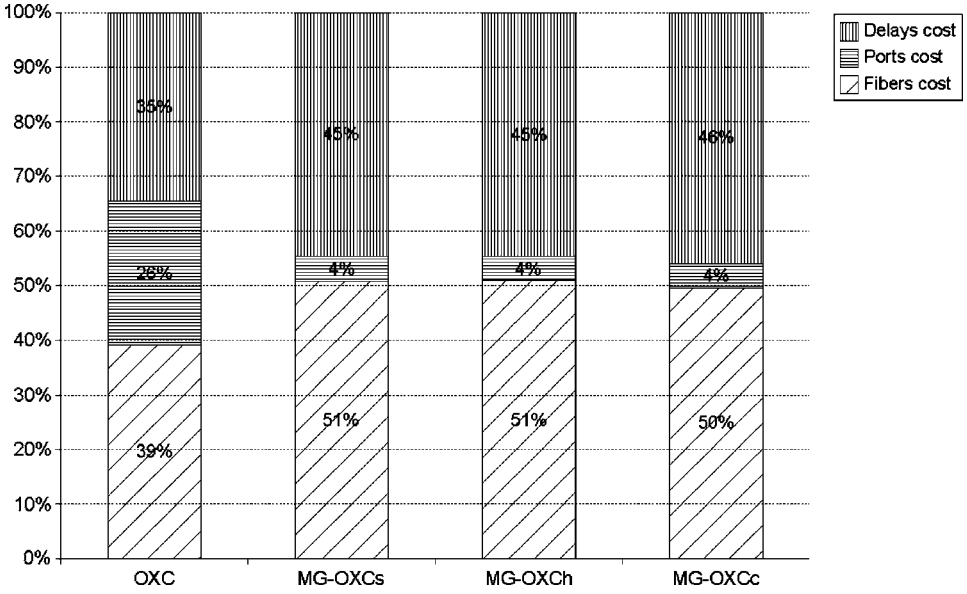

Fig. 5. Cost distribution for EONc-3 in different grouping cases.

6. Conclusions

In this work we analyzed and quantified, for the first time to our knowledge, the effect of joint end-to-end and subpath wavebanding in optical networks, carrying on a cost-effective design of wide-area case-study networks. We proposed and applied ILP formulations for a case-by-case analysis and showed the benefits of WBS technology when switching operates at wavelength, waveband, and fiber levels. The best results for both network cost and port number are achieved by means of subpath wavebanding; in particular we showed that the application of end-to-end wavebanding by itself already leads to very good results, not far from the results achievable by subpath grouping, especially for high loads; secondarily, subpath grouping with heterogeneous grouping does not introduce relevant savings with respect to the case without heterogeneous grouping.

Globally we showed that a WBS backbone can be less expensive by up to 22% and can save more than 50% of ports in comparison with classical OXC-based networks. Further work is needed to develop heuristics for the design of WBS networks with subpath grouping in order to apply this technique to dense networks.

Acknowledgments

This work was partially supported by EU Information Society Technologies (IST) Network of Excellence e-Photon/One.

References

1. X. Cao, V. Anand, and C. Qiao, "Waveband switching in optical networks," Commun. Mag. **41**(4), 105–112 (2003).
2. P.-H. Ho, H. T. Mouftah, and J. Wu, "A scalable design of multigranularity optical cross-connects for the next-generation optical Internet," IEEE J. Sel. Areas Commun. **21**, 1133–1142 (2003).
3. A. Kolarov, T. Wang, B. Sengupta, and M. Cvijetic, "Impact of waveband switching on dimensioning multi-granular hybrid optical networks," in *Proceedings of Optical Network Design and Modeling (ONDM 2005)* (IEEE, 2005), pp. 371–381.
4. M. Lee, J. Yu, Y. Kim, C. Kang, and J. Park, "Design of hierarchical crossconnect WDM networks employing a two-stage multiplexing scheme of waveband and wavelength," IEEE J. Sel. Areas Commun. **20**, 166–171 (2002).
5. Y. Shun, O. Canhui, and B. Mukherjee, "Design of hybrid optical networks with waveband and electrical TDM switching," in *Proceedings of Global Telecommunications Conference (GLOBECOMM 2003)* (IEEE, 2003), Vol. 5 pp. 2803–2808.
6. S. Secci and B. Sansó, "Design and dimensioning of a novel composite-star WDM network with TDM channel partitioning," in *Proceedings of Third International Conference on Broadband Networks (Broadnets 2006)* (IEEE, 2006).
7. *Wikipedia, the Free Encyclopedia*, http://en.wikipedia.org/wiki/Metropolitan_cities_of_Europe, and *United States Census 2000 Population and Housing*, http://www.census.gov/main/www/cen2000.html.
8. "Interfaces for the Optical Transport Networks (OTN)," G.709/Y.1331, ITU-T International Communication Union, March 2003.
9. G. Maier, A. Pattavina, and M. Tornatore, "WDM network optimization by ILP models based on flows aggregation," IEEE/ACM Trans. Netw. (to be published).
10. G. Maier, A. Pattavina, S. De Patre, and M. Martinelli, "Optical network survivability: protection techniques in the WDM layer," Photonic Netw. Commun. **4**, 251–269 (2002).